地上では持ち上がらない下肢を水面近くまで上げることが出来る）

- 水には抵抗もある（動かす速度を調整するだけで負荷を変更することが出来る、体の向きを変えるだけでも抵抗は変わる）
- 水には圧力もある（水圧によって水中にいるだけで胸郭に圧がかかっており、それだけで呼吸筋のトレーニングになる、下肢の方が圧は高いので心臓への循環は容易である）
- 水は冷たい（体温調節機構のトレーニングにもなる、ただし繰り返した場合）
- 転倒しても怪我をしにくい

水中運動の欠点

- 着替えなどが面倒
- 循環器系に異常があると負担がかかりすぎる可能性がある
- もともと水中運動に慣れ親しんでない人に対してアピール度が少ない
- 本当に運動能力が向上するかどうかのエビデンスがない

運動を行うことで、減量や体脂肪減少が期待されるが、今回の研究ではどちらも達成されなかった。特にE群では逆に体脂肪率の上昇を認め、しかも男女とも同様の変化であったことから、トレーニングマシンを用いた場合の普遍的な変化である可能性が高い。水中では寒冷刺激のため脂肪は減少しにくいが、歩行に比べて機器トレーニングの方がより寒冷の影響を受けやすい可能性が考えられた。

筋力は、E群においては下肢・上肢ともに筋力が上昇し、その効果は筋力の弱い女性においてより顕著に認められた。C群においても水中歩行を繰り返した効果で、膝伸展筋力が向上したものと思われるが、水中歩行では上肢筋力を高めるような動作がほとんどないため、握力は増大しなかったものと推察する。

歩行速度は両群とも速くなっていたが、有意ではなく、片脚起立時間は両群とも変動を認めなかった。歩行速度測定は、最大速度で5mという設定のみで行っており、測定方法に問題があった可能性もある。片脚起立時間は60秒を限度として測定したため、60秒という記録を示した被験者が、両群合わせて10名もいたことから、効果検出力が弱かった可能性がある。

柔軟性の指標としてファンクショナルリーチの測定を行ったが、両群とも有意な改善を示し、特にどちらの訓練方法がよいという指標にはならなかった。タンデムゲイトも同様に身体動揺性の指標として採用したが、ほとんど全員が2mの直線を揺れることなく歩ききっており、健康な高齢者を対象とした場合には重要な意味を持たない項目ではないかと考えられた。

踵骨の骨量は、両群とも明らかに増加しており、いずれの方法でも骨代謝に刺激を与えた可能性が考えられる。しかし、これまでの研究では、踵に衝撃が加わるような運動の場合にのみ骨量が増加したと報告されている[6]。水中の運動では、器具を用いても用いなくても、踵への衝撃力は強くないと考えられ、今回の骨量改善効果の機序に関してはさらなる研究が必要である。

水中運動により血圧が低下することは、水圧により下肢の循環血液が心臓に戻りやすいことから説明できる。これまでにも水中運動により血圧が低下することは報告されている[7]が、今回の研究でも実証された。しかし、E群においては血圧の低下は有意では

なく、その理由として、マシンを使用しての運動では無酸素運動状態になっている時間が多いためではないかと推測された。両群とも心拍数は有意に上昇しており、運動負荷としては十分と考えられた。

今回の結果から、水中トレーニングマシンは下肢だけではなく、上肢の筋力も向上させることが可能で、循環系に過度の負荷をかけずに訓練を行うことが可能であることが判明した。現状の形態であっても高齢者の運動プログラムに充分利用可能であると思われる。2005年11月時点で、我が国で本システムが導入されているのは、灘浜ガーデンバーデンを含めて6カ所しかない。普及率が悪いのは、価格とともにサイズが大きいことが挙げられる。今回の研究により、その効果は十分に証明されたので、今後はダウンサイジングを含めた改良を行いたいと考えている。

なお、本研究はクロスオーバー法にて実施しており、現在は両群の実施項目を入れ替えて同様の研究を行っている。

謝辞

本研究に施設を提供するとともに、多大なご協力をいただいた灘浜ガーデンバーデンに深謝します。また、長期間にわたり、我々の研究に参加していただいた被験者の皆さんにお礼申し上げます。測定に御協力いただいた中土保・折戸芳紀・赤松波子・加藤良一（以上大阪市立大学大学院医学研究科リハビリテーション部）・遠藤芳恵（大阪市立弘済院付属病院）の諸氏とトレーナーとして参加した山本聖人（大阪産業大学）に感謝します。

なお、本研究は平成17年度石本記念デサントスポーツ科学振興財団の研究助成を受けて行われた。ここに記して感謝の意を表する。

参考文献

1) Pritchett AM, Foreyt JP, Mann DL: Treatment of the metabolic syndrome: the impact of lifestyle modification. *Curr Atheroscler Rep.* 2005 Mar;7(2):95-102
2) de Jong Z, Vlieland TP: Safety of exercise in patients with rheumatoid arthritis. *Curr Opin Rheumatol.* 2005 Mar;17(2):177-82
3) Eckerson J, Anderson T: Physiological response to water aerobics. *J Sports Med Phys Fitness.* 1992 Sep;32(3):255-61
4) Eyestone ED, Fellingham G, George J, Fisher AG: Effect of water running and cycling on maximum oxygen consumption and 2-mile run performance. *Am J Sports Med.* 1993 Jan-Feb;21(1):41-4.
5) Frangolias DD, Rhodes EC: Metabolic responses and mechanisms during water immersion running and exercise. *Sports Med.* 1996 Jul;22(1):38-53.
6) Lehtonen-Veromaa M, Mottonen T, Kautiainen H, Heinonen OJ, Viikari J: Influence of physical activity and cessation of training on calcaneal quantitative ultrasound measurements in peripubertal girls: a 1-year prospective study. *Calcif Tissue Int.* 2001 Mar;68(3):146-50.
7) Pump B, Shiraishi M, Gabrielsen A, Bie P, Christensen NJ, Norsk P: Cardiovascular effects of static carotid baroreceptor stimulation during water immersion in humans. *Am J Physiol Heart Circ Physiol.* 2001 Jun;280(6):H2607-15.

表　参加者の開始時プロフィールと身体計測値
両群間にすべての項目で有意差を認めなかった

	コントロール群	水中エクササイズ群
人数(n)	14	14
年齢(y)	62.1±7.4	63.9±6.3
女性比率(%)	50	57
身長(cm)	163.9±8.6	160.3±61.9
体重(Kg)	65.4±11.3	62.8±8.3
体脂肪率(%)	26.3±7.4	26.7±9.2
アームスパン(cm)	162.6±9.6	159.4±7.6
過去一年の転倒回数（回）	0.21±0.80	0.31±0.86
継ぎ足歩行（歩数）	7.9±2.6	8.4±1.6
歩行速度（秒/5 m）	2.6±0.8	2.4±0.5
片脚起立時間（秒）	37.6±22.5	36.3±19.8
ファンクショナルリーチ(cm)	35.1±7.6	31.6±5.4
握力(Kg)	30.6±7.8	28.9±7.7
膝伸展力(N)	285.1±63.4	290.2±51.3
踵骨 SOS(m/s)	1494.9±25.8	1483.8±23.7

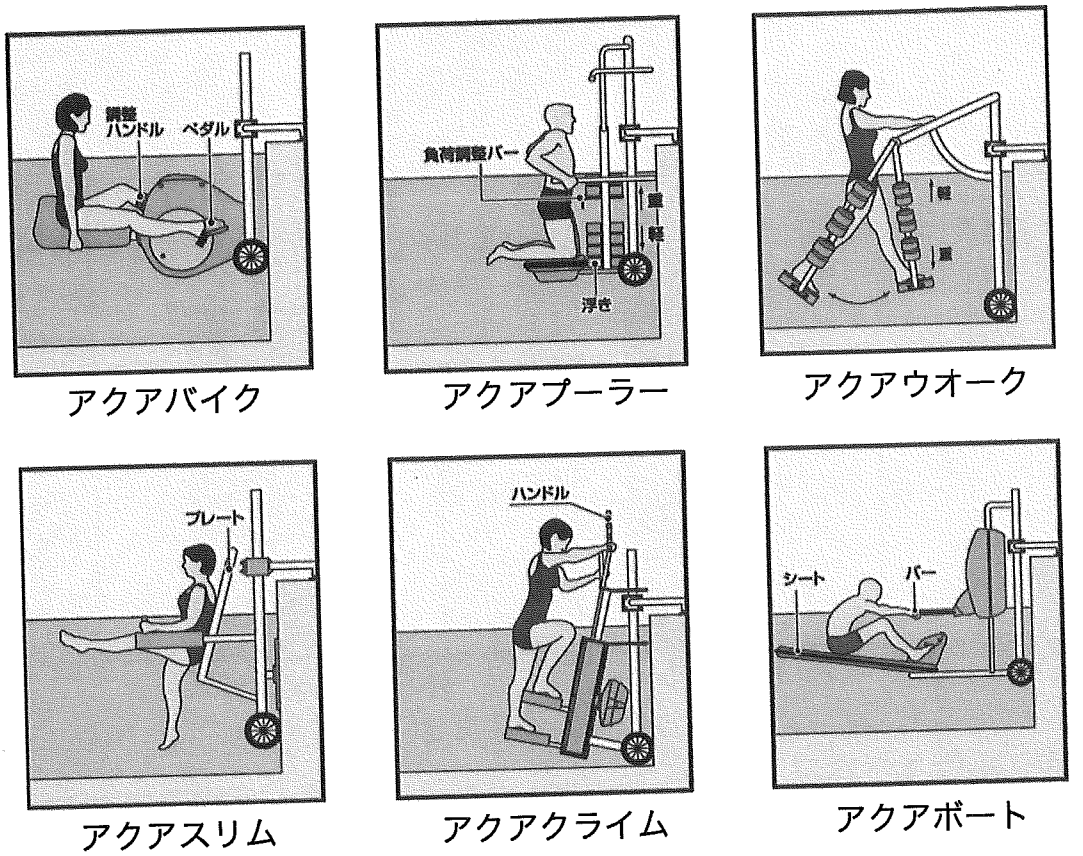

図1　使用水中トレーニングマシン
ダイレオホームページ http://www.daileo.co.jp/home/home.htmより転載

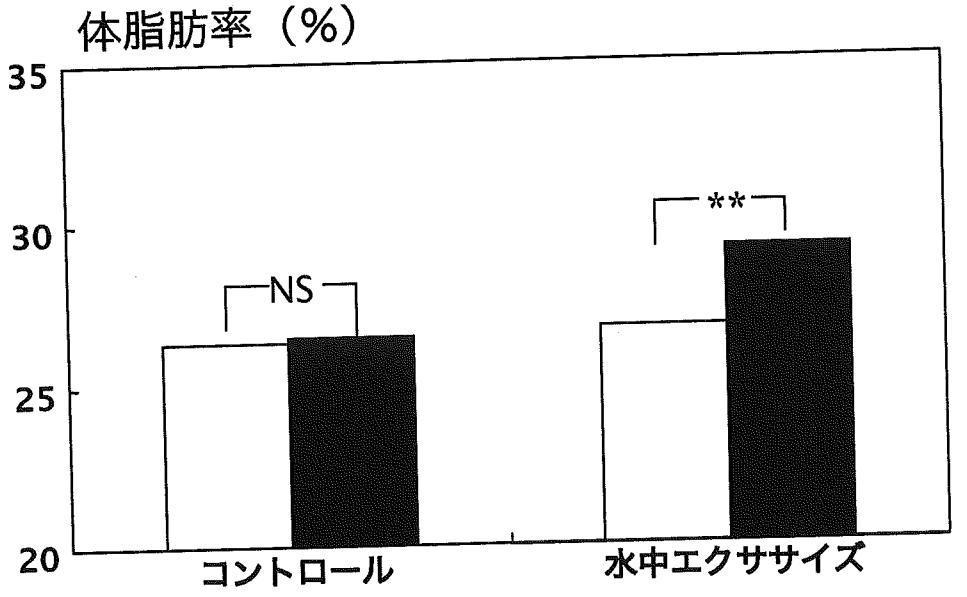

図2　体脂肪率の変化
白抜きが開始時、黒カラムが10週後。NS: not significant, ** : P<0.01

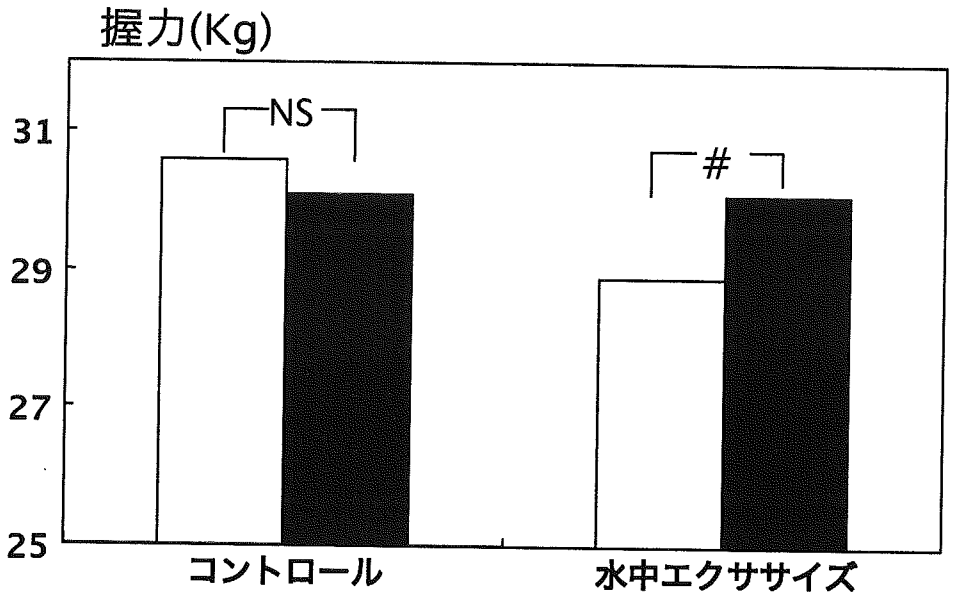

図3　非利き手握力の変化
白抜きが開始時、黒カラムが10週後。NS: not significant, # P=0.06

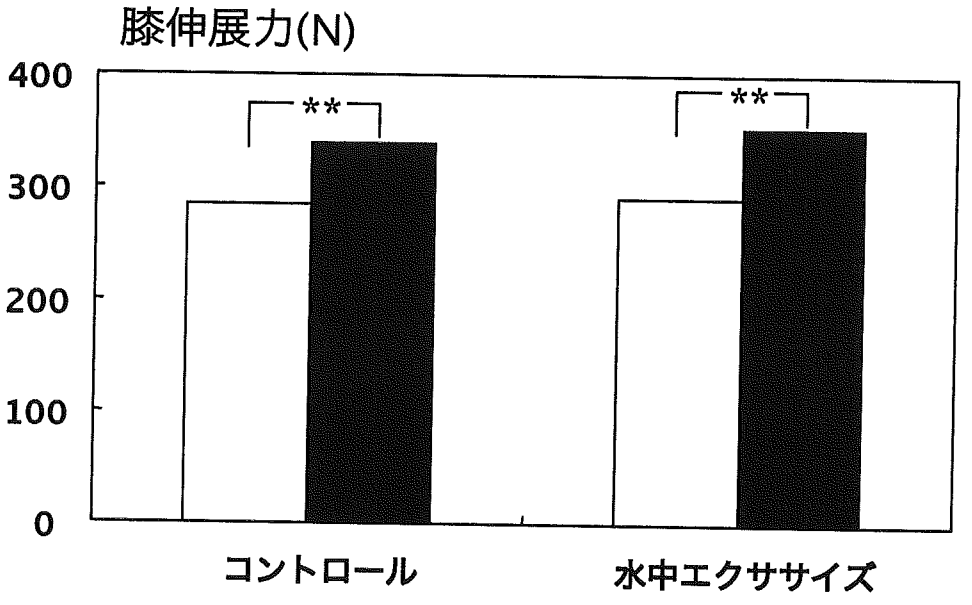

図4　膝伸展力の変化
白抜きが開始時、黒カラムが10週後。**：P<0.01

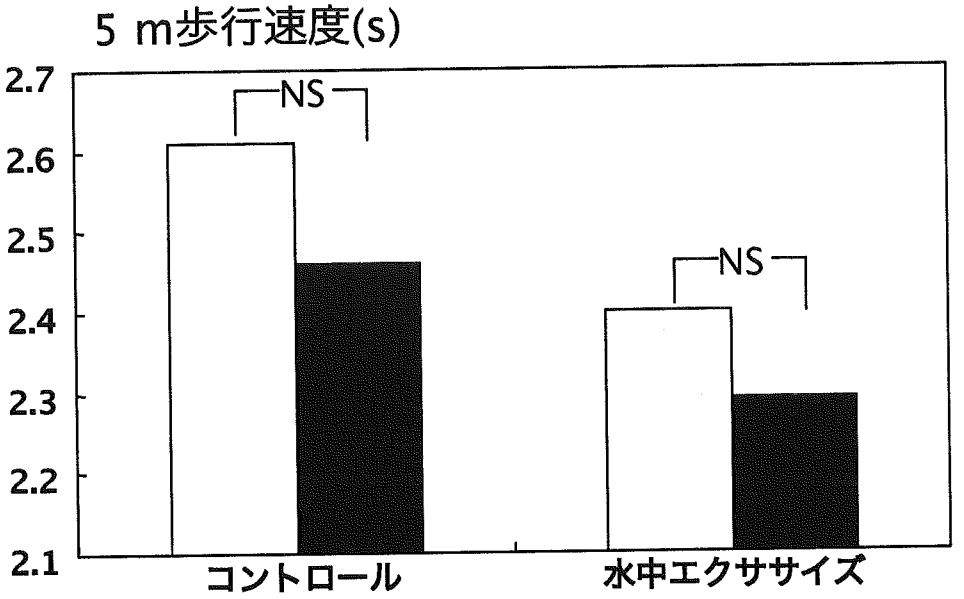

図5　5 m歩行速度
白抜きが開始時、黒カラムが10週後。NS: not significant

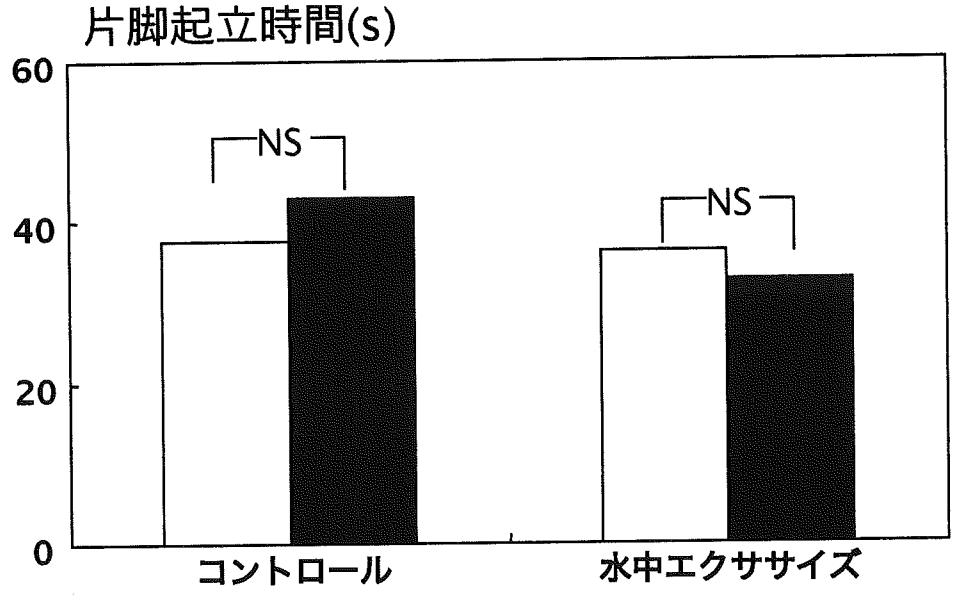

図6　片脚起立時間の変化
白抜きが開始時、黒カラムが10週後。NS: not significant

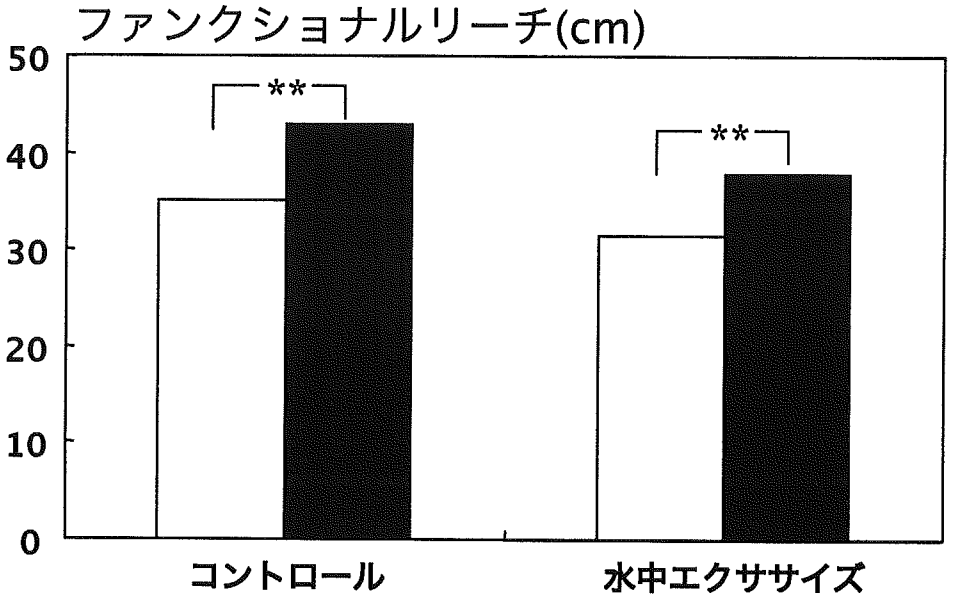

図7　ファンクショナルリーチの変化
白抜きが開始時、黒カラムが10週後。**：P<0.01

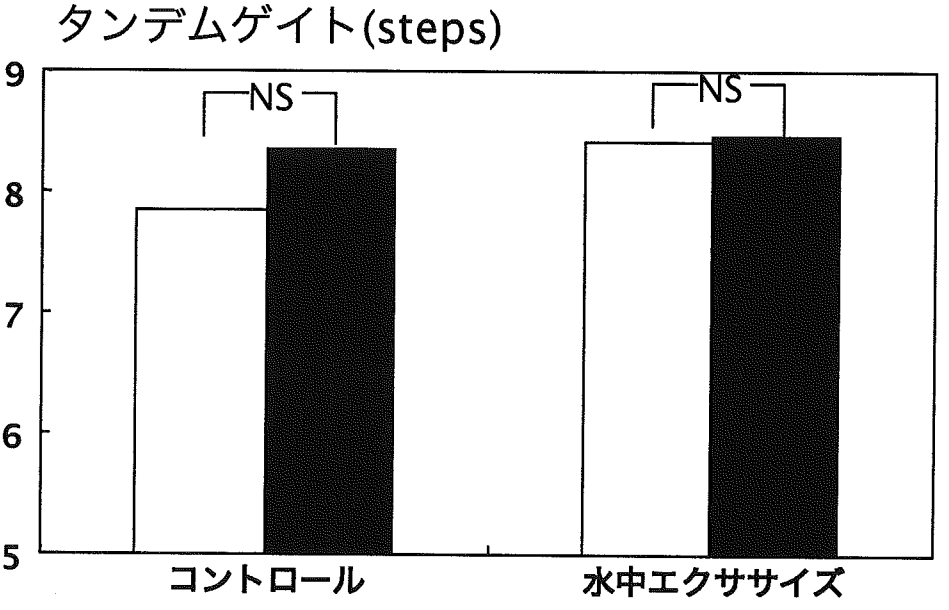

図8　タンデムゲイトの変化
白抜きが開始時、黒カラムが10週後。NS: not significant

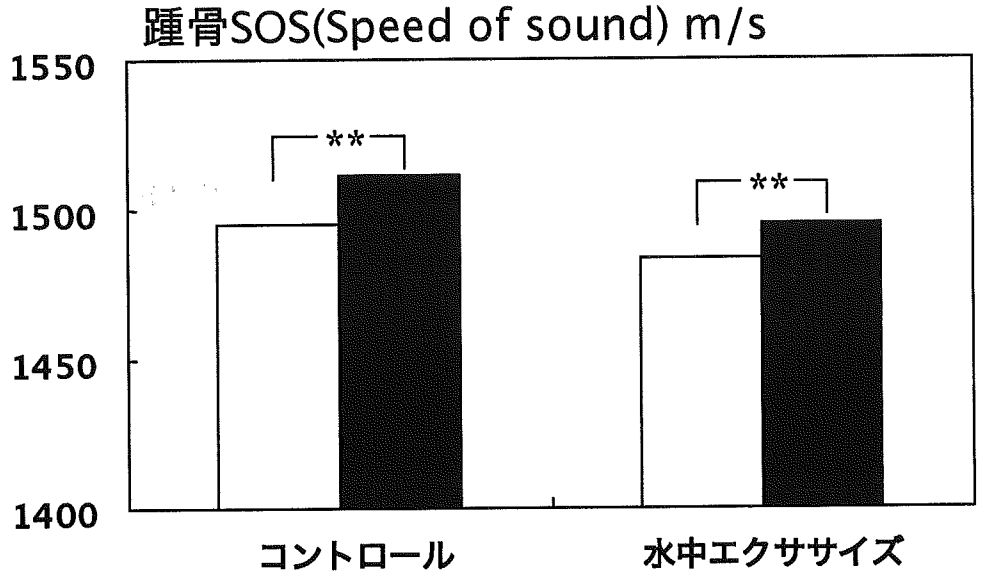

図9　踵骨骨量の変化
白抜きが開始時、黒カラムが10週後。**：P<0.01

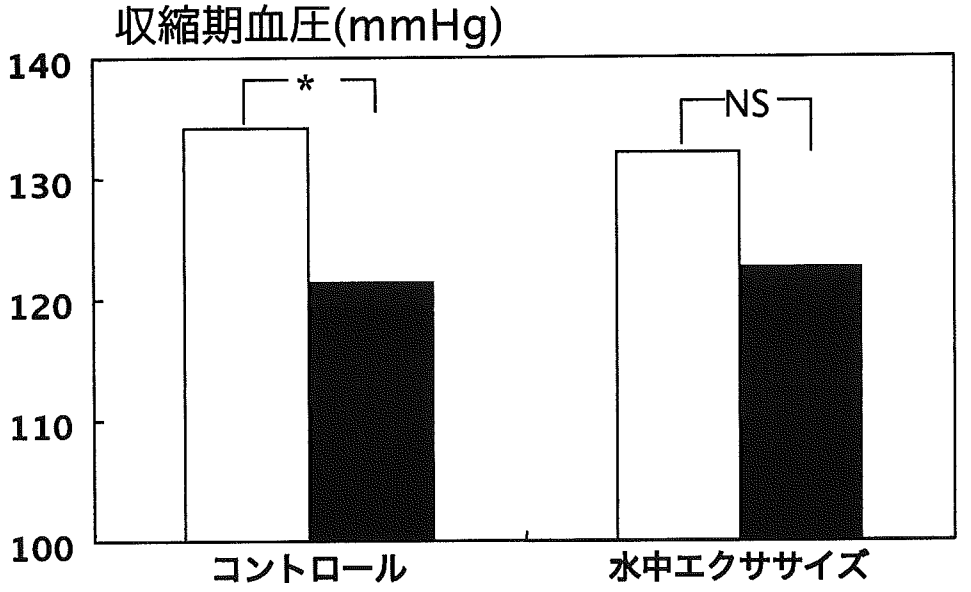

図10　トレーニング前後の収縮期血圧の変化
白抜きが開始時、黒カラムが10週後。NS: not significant, *：P<0.01

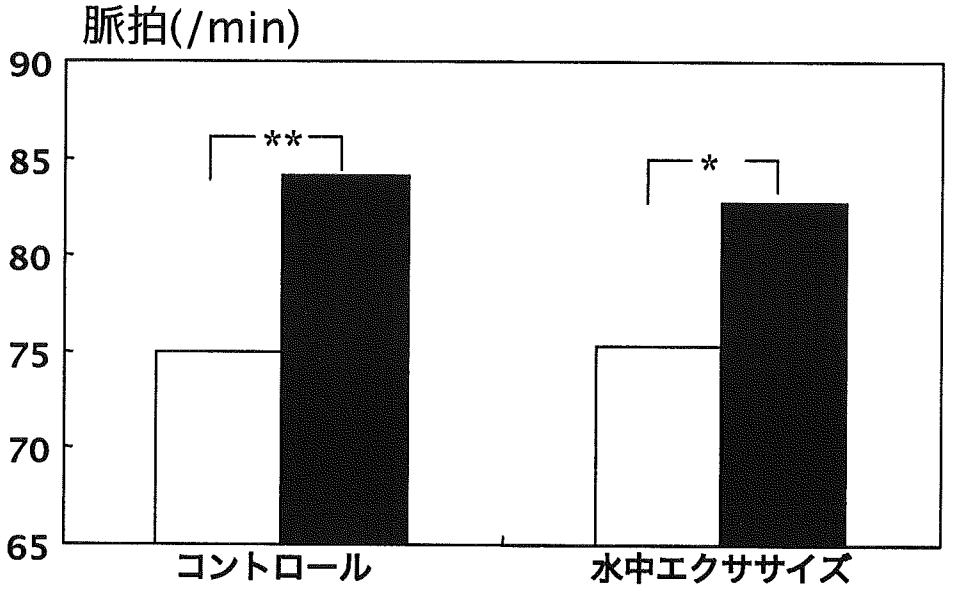

図11　トレーニング前後の脈拍の変化
白抜きが開始時、黒カラムが10週後。*: P<0.05, ** : P<0.01

Ⅲ. 研究成果の刊行に関する一覧表

発表者氏名	論文タイトル名	発表誌名	巻号	ページ	出版年
Toyoda H, Terai H, Sasaoka R. Oda K, Takaoka K	Augmentation of bone morphogenetic protein-induced bone mass by local delivery of a prostagrandin E EP-4 receptor agonist	Bone	37	555-562	2005
Nawata M, Wakitani S, Nakaya H, Tanigami A, Seki T, Nakamura Y, Saito N, Sano K, Hidaka E, Takaoka K	Use of bone morphogenetic protein 2 and diffusion chambers to engineer cartilage tissue for the repair of defects in articular cartilage.	Arthritis & Rheum	52	155-163	2005
Masahiro Yoneda, Hidetomi Terai, Yuuki Imai, Takao Okada, Kazutoshi Nozaki, Hikaru Inoue, Shimpei Miyamoto, Kunio Takaoka	Repair of an Intercalated Long Bone Defect with a Synthetic Biodegradable Bone-inducing Implant.	Biomaterials	26	5145-5152	.2005
Takashi Namikawa, Hidetomi Terai, Eisuke Suzuki, Masatoshi Hoshino, Hiromitsu Toyoda, Hiroaki Nakamura, Shimpei Miyamoto, Naoyuki Takahashi, Tadashi Ninomiya, Kunio Takaoka	Experimental Spinal Fusion with Recombinant Human Bone Morphogenetic protein-2 Delivered by a Synthetic Polymer and Beta-Tricalcium Phosphate in a Rabbit Model	Spine	30	1717-1722	2005
Tada M., Inui K., Koike T., Takaoka K.	Use of local electroporation enhances methotrexate effects with minimum dose in ajuvant-induced arthritis.	Arthritis Rheum	52	637-641	2005
Ito Y, Sakai T, Tomo H, Nakao Y, Inui K, Koike T, Nakatsuchi T, Takaoka K.	Computerized assessment of Bankart lesions under tension with magnetic resonance arthrography.	J Shoulder Elbow Surg.	14	247-251	2005
Nakatsuchi T., Otani M., Osugi H., Koike T	The necessity of chest physical therapy for thoracoscopic oesophagectomy.	The Journal of International Medical Research	33	434-441	2005
H. Toyoda, Y. Ito, H. Tomo, Y. Nakao, T. Koike, K. Takaoka	Evaluation of rotator cuff tears with magnetic resonance arthrography.	Clin Ortho Related Res	439	109-115	2005
小池達也、高岡邦夫	BMPs 薬理作用と生理作用-骨形成促進作用-	日本臨床	63	426-430	2005
小池達也	WHOテクニカルレポートをめぐって 運動についての評価	Clinical Calcium	15	673-677	2005
渡邊具子、折戸芳紀、豊田宏光、洲鎌亮、多田昌弘、高岡邦夫、小池達也	ヒッププロテクターによる大腿骨頸部/転子部骨折の予防	整形外科看護	11	298-304	2006
渡邊具子、折戸芳紀、豊田宏光、洲鎌亮、多田昌弘、高岡邦夫、小池達也	ヒッププロテクターによる腿骨頸部骨折の予防	Osteoporosis Japan	14	88-90	2006
小池達也	ヒッププロテクターによる大腿骨頸部骨折の予防	Geriatric Medicine	44	187-193	2006
小池達也、折戸芳紀、多田昌弘、洲鎌亮、豊田宏光、小林千益、高岡邦夫	ヒッププロテクターは大腿骨頸部骨折ハイリスク集団の頚部骨折を抑制する	Osteoporosis Japan	14	42-45	2006
小林千益、久保俊一、高岡邦夫	特発性大腿骨頭壊死症に対する人工関節置換術の成績：人工骨頭置換術との比較.	別冊整形外科	48	173-177	2005
堀内博志、五明広樹、中島滋郎、若林真司、斎藤直人、小林千益、縄田昌司、橋本博史、津田裕士、深沢徹、谷口俊一郎、高岡邦夫	特発性大腿骨頭壊死症におけるグルココルチコイド受容体の遺伝子多型解析	別冊整形外科	48	51-53	2005

Ⅳ. 研究成果の刊行物・別冊

OsteoArthritis and Cartilage (2005) **13,** 405–417

doi:10.1016/j.joca.2004.12.014

Osteoarthritis and Cartilage | ICRS International Cartilage Repair Society | OA OSTEOARTHRITIS

A new biotechnology for articular cartilage repair: subchondral implantation of a composite of interconnected porous hydroxyapatite, synthetic polymer (PLA-PEG), and bone morphogenetic protein-2 (rhBMP-2)

Noriyuki Tamai M.D., Ph.D.†, Akira Myoui M.D., Ph.D.†, Makoto Hirao M.D.†, Takashi Kaito M.D.†, Takahiro Ochi M.D., Ph.D.‡, Junzo Tanaka Ph.D.§, Kunio Takaoka M.D., Ph.D.|| and Hideki Yoshikawa M.D., Ph.D.†*

† *Department of Orthopaedic Surgery, Osaka University Graduate School of Medicine, 2-2 Yamadaoka, Suita, Osaka 565-0871, Japan*

‡ *National Hospital Organization Sagamihara National Hospital, 18-1 Sakuradai, Sagamihara, Kanagawa 228-8522, Japan*

§ *Biomaterials Center, National Institute for Materials Science, 1-1 Namiki, Tsukuba, Ibaraki 305-0044, Japan*

|| *Department of Orthopaedic Surgery, Osaka City University Medical School, 1-4-3 Asahimachi, Abeno-ku, Osaka 545-8585, Japan*

Summary

Objective: Articular cartilage repair remains a major obstacle in tissue engineering. We recently developed a novel tool for articular cartilage repair, consisting of a triple composite of an interconnected porous hydroxyapatite (IP-CHA), recombinant human bone morphogenetic protein-2 (rhBMP-2), and a synthetic biodegradable polymer [poly-D,L-lactic acid/polyethylene glycol (PLA-PEG)] as a carrier for rhBMP-2. In the present study, we evaluated the capacity of the triple composite to induce the regeneration of articular cartilage.

Methods: Full-thickness cartilage defects were created in the trochlear groove of 52 New Zealand White rabbits. Sixteen defects were filled with the bone morphogenetic protein (BMP)/PLA–PEG/IP-CHA composite (group I), 12 with PLA–PEG/IP-CHA (group II), 12 with IP-CHA alone (group III), and 12 were left empty (group IV). The animals were killed 1, 3, and 6 weeks after surgery, and the gross appearance of the defect sites was assessed. The harvested tissues were examined radiographically and histologically.

Results: One week after implantation with the BMP/PLA–PEG/IP-CHA composite (group I), vigorous repair had occurred in the subchondral defect. It contained an agglomeration of mesenchymal cells which had migrated from the surrounding bone marrow either directly, or indirectly via the interconnecting pores of the IP-CHA scaffold. At 6 weeks, these defects were completely repaired. The regenerated cartilage manifested a hyaline-like appearance, with a mature matrix and a columnar organization of chondrocytes.

Conclusions: The triple composite of rhBMP-2, PLA-PEG, and IP-CHA promotes the repair of full-thickness articular cartilage defects within as short a period as 3 weeks in the rabbit model. Hence, this novel cell-free implant biotechnology could mark a new development in the field of articular cartilage repair.

Key words: Articular cartilage repair, Interconnected porous hydroxyapatite (IP-CHA), BMP, PLA-PEG.

Introduction

To date, the myth "once destroyed, cartilage cannot be repaired" has yet to be dispelled[1]. Mature articular cartilage cannot heal spontaneously owing to its low mitotic activity, which contrasts to the rapid rate of chondrocytic mitosis during normal cartilage growth.

Recently, several researchers have attempted to utilize culture-expanded autologous chondrocytes in combination with collagen sponges or fibrin glue to effect the repair of cartilage defects[2,3]. However, the results were either unsatisfactory or, if satisfactory, were achieved only after a lengthy wait for the regeneration of hyaline cartilage[2,4]. These poor results may reflect the characteristics of the transplantation technique, which involves the application of cartilage-derived cells to the defect[5].

Mesenchymal stem cells (MSCs) isolated from bone marrow have the ability to differentiate into chondrocytes, osteoblasts and other connective tissue cells of mesenchymal origin when cultured under appropriate *in vitro* conditions[6,7]. In an effort to exploit the pluripotentiality of MSCs, MSC-based repair strategies have been instigated in rabbits and goats, but with limited success[8,9]. Clinically,

*Address correspondence and reprint requests to: Hideki Yoshikawa. Tel: 81-6-6879-3552; Fax: 81-6-6879-3559; E-mail: yhideki@ort.med.osaka-u.ac.jp
Received 8 November 2004; revision accepted 20 December 2004.

surgical interventions, such as microfracturing, abrasion arthroplasty and osteochondral drilling, have been widely used and considered to be partially successful[10,11]. These techniques are based on the concept that intentional damage to the subchondral bone recruits MSCs to the defect, thereby promoting cartilage repair.

A potentially powerful alternative approach for cartilage regeneration is the local administration of bone morphogenetic proteins (BMPs), which are members of the transforming growth factor-β superfamily. BMPs have been shown to regulate and promote the growth and differentiation of chondrocytes, osteoblasts and MSCs[12,13]. Indeed, recombinant human bone morphogenetic protein-2 (rhBMP-2) can stimulate the *in vitro* synthesis of components of the chondrocytic matrix, such as proteoglycans and type-II collagen[14–16]. Furthermore, BMPs are known to induce the condensation of MSCs when administered *in vivo*[17–19].

Inorganic biomaterials, such as carbon fibers[20], collagen scaffolds[2,21], absorbable polymers[22,23], and hydroxyapatite[24,25], have been used for articular cartilage repair. Some success has been achieved in the repair of small osteochondral defects, but no widely accepted method exists for the complete healing of hyaline cartilage. The cause of the failure lies not in the nature of the biomaterial itself but in its structure, which is not regulated three-dimensionally.

In the present study, we attempted to combine two distinct approaches: the strong induction of subchondral bone regeneration, with a view to recruiting bone-marrow MSCs to the osteochondral defect; and the appropriate local delivery of rhBMP-2 to induce chondrocytic differentiation and to stimulate matrix production by the chondrocytes. To instigate these two approaches simultaneously, we developed a combined biomaterial, which consists of a synthetic hydroxyapatite with an interconnected porous structure (IP-CHA), and a synthetic bioabsorbable polymer, namely, PLA–PEG (poly-D,L-lactic acid–polyethylene glycol block copolymer). In this system, PLA–PEG serves as a drug-delivery carrier, which permits the ideal release of rhBMP-2 over a period of about 3 weeks[26–29]. IP-CHA is made from hydroxyapatite, which is a bioactive ceramic with osteoconductive properties[30,31]. In addition, IP-CHA has a finely organized, three-dimensional interconnecting pore structure. The material is highly porous (porosity: 75%) and the pore size (150 μm) is appropriate for bone formation. The large interconnecting channels (average diameter: 40 μm) permit the easy penetration of tissue into the deep pores[30]. Owing to these structural properties, IP-CHA can itself induce local bone repair processes[30,32,33]. The interconnecting pore structure of the material also permits its easy impregnation with cytokines or growth factors borne by an appropriate delivery system.

The rationale behind the selection of key experimental design parameters was as follows: Skeletally immature adolescent rabbits (4–6 months old and 2.5–3.0 kg in weight) were selected because the ability of articular cartilage to repair depends mostly on the bone-marrow MSCs, which are metabolically more active and have a higher capacity to induce repair in an immature model. The decision to use full-thickness defects with a diameter of 4 mm and a depth of 6 mm was based on the results of previous studies. In rabbits, partial-thickness defects do not heal spontaneously, whereas full-thickness ones with a diameter less than 3 mm do, and the repair tissue is composed either of hyaline- or of fibrocartilage[34–36]. Hence, it was necessary to establish a model in which this upper limit for spontaneous repair was exceeded.

In the present study, we demonstrate the capacity of the triple composite of rhBMP-2, PLA-PEG, and IP-CHA to effect articular cartilage repair. The goal was to achieve the repair of full-thickness articular cartilage defects in rabbits in as short a time as possible, with the ultimate view of inducing the repair of similar lesions in humans; specifically, those generated during osteoarthritis, rheumatoid arthritis, and osteochondritis dissecans.

Materials and methods

PREPARATION OF IMPLANTS

IP-CHA was synthesized by Toshiba Ceramics Co., Ltd. (Kanagawa, Japan), as previously described[30]. In short, we adopted a "foam gel" technique, which involves two unique steps: a foaming step and a crosslinking step. During the foaming step, the hydroxyapatite slurry is mixed with a foaming agent (polyethyleneimine, 40% by weight). During the crosslinking (polymerization) step, the foam-like hydroxyapatite slurry is rapidly gelatinized using a water-soluble crosslinking agent (a poly-functional epoxy compound)[30].

rhBMP-2, which is produced by the Genetics Institute (Cambridge, MA) and was given to us by Yamanouchi Pharmaceutical Co., Ltd. (Ibaraki, Japan), was dissolved in buffer (5 mM glutamic acid, 2.5% glycine, 0.5% sucrose, and 0.01% Tween 80) at a concentration of 1 mg/ml. The solution was then filter-sterilized. Two-hundred mg of PLA–PEG [molecular weight (MW) = 11,400, dispersity (Mw/Mn) = 1.1 (Taki Chemical Research Laboratory, Kanagawa, Japan)] was dissolved in 1 ml of acetone. To prepare a single implant sample, a 25 μl aliquot of the PLA–PEG mass (5 mg) was mixed with a 20 μl sample of rhBMP-2 (20 μg). The specimen of IP-CHA (4 mm in diameter and 4 mm in height) was immersed in the mixture and the solvent was evaporated in a centrifuge/evaporator. The resulting BMP/PLA–PEG/IP-CHA composite was sterilized with ethylene oxide gas for 24 h on the day preceding implantation.

IN VITRO RELEASE KINETICS OF RHBMP-2

The release of rhBMP-2 from the BMP/PLA–PEG/IP-CHA composite was measured using a quantitative sandwich enzyme immunoassay technique (AN'ALYZA®; BMP-2 immunoassay, TECHNE Co. MN, USA). The dose of rhBMP-2 used in the *in vivo* experiments (20 μg) was chosen for the release study. Twelve BMP/PLA–PEG/IP-CHA composites, which were prepared in the same way as those used for implantation in the rabbit model, were placed within 24-well plates together with 500 μl of phosphate-buffered saline [(PBS) Sigma] and incubated for 21 days at 37°C. The supernatant was removed and replaced with fresh PBS every day. The supernatants removed on days 1, 3, 7, 14 and 21 were analyzed for their concentrations of rhBMP-2 according to the enzyme-linked immunosorbent assay (ELISA) technique. The bioactivity of the composites maintained *in vitro* for 0, 7 and 21 days (four samples per time point) was also assessed (see next section).

IN VIVO BIOASSAY FOR THE BMP/PLA–PEG/IP-CHA COMPOSITE

To assess the biological activity of composites that were maintained *in vitro* for 0, 7 and 21 days, these, as well as

IP-CHAs without rhBMP-2 (controls), were implanted within the back muscles of 5-week-old male JCL: ICR mice (one composite per animal; four mice per group, i.e., control, day 1, day 7 and day 21) as previously reported[27,28]. The implants were harvested 2 weeks after implantation. They were then crushed, homogenized in 0.2% Nonidet P-40 containing 1 mM $MgCl_2$, and centrifuged at 10,000 rpm for 1 min at 4°C. The supernatants were assayed for alkaline phosphatase (ALP) activity using *p*-nitrophenyl phosphate as a substrate. The product was measured spectrophotometrically at an absorption wavelength of 410 nm ($n = 4$ per group)[37].

ANIMAL EXPERIMENTS

Fifty-two New Zealand White rabbits weighing 2.5–3.0 kg (4–6 months) were kept in cages and had free access to food pellets and water. The rabbits were anesthetized by the intravenous injection of 1 ml of pentobarbital [50 mg/ml (Nembutal®; Dainippon Pharmaceutical Co. Ltd., Osaka, Japan)] and the intramuscular injection of 1 ml of xylazine hydrochloride [25 mg/ml (Seractal®; Bayer, Germany)]. After shaving, disinfection, and draping, a straight 3-cm long medial parapatellar incision was made over the right knee and the patella was everted. Full-thickness articular osteochondral defects, 4 mm in diameter and 6 mm in depth, were created mechanically in the patellar groove of the right distal femur. Rabbit knees were divided into four implant groups: group I ($n = 16$ knees) received the BMP/PLA–PEG/IP-CHA composite; group II ($n = 12$ knees) received the PLA–PEG/IP-CHA composite (no rhBMP-2), group III ($n = 12$ knees) received IP-CHA alone; and group IV ($n = 12$ knees) underwent a sham operation with no implantation. In groups I, II, and III, all implants were placed at the subchondral bone level, 2 mm beneath the surface of the adjacent cartilage. The fascial layer was closed with absorbable sutures, and the skin with 4-0 nylon sutures. One week after surgery, four rabbits in group I were killed. At 3 weeks, 24 rabbits were killed (group I = 6, group II = 6, group III = 6, group IV = 6), and at 6 weeks 24 rabbits were killed (group I = 6, group II = 6, group III = 6, group IV = 6). The animals were killed by an intravenous injection of 5 ml of pentobarbital (Table I). All animal experiments were approved by the Animal Laboratory, Faculty of Medicine, Osaka University, Japan.

RADIOGRAPHIC AND HISTOLOGICAL EVALUATIONS

The harvested tissues were radiographed using a soft X-ray apparatus [35 kV; 300 μA; 300 s; MX20 (Faxitron X-ray Co., IL, USA)] and then fixed in 4% paraformaldehyde (pH 7.4) for 48 h at 4°C. Tissue samples were decalcified in 20% ethylenediaminetetraacetic acid (pH 7.4) at 4°C, dehydrated in a graded ethanol series and embedded in paraffin. Serial sections (5 μm in thickness) were cut sagittally through the center of the operative site and stained with hematoxylin and eosin (H&E) or with safranin-O. For the immunohistochemical analysis, paraffin sections were treated with 3% H_2O_2 to block endogenous peroxidase activity. They were pretreated with serum to block non-specific staining. The sections were then incubated with mouse monoclonal antibodies: anti-type-I collagen (I-8H5, Daiichi Fine Chemical Co., Ltd, Toyama, Japan), anti-type-II collagen (II-4C11, Daiichi Fine Chemical Co., Ltd, Toyama, Japan), and anti-CD105 [(Endoglin) 555722, BD Bioscience, NJ, USA]; and with the polyclonal antibody goat anti-Cbfa1 [(Runx2) C-19, Santa Cruz, CA, USA][38]. The specimens were treated with the appropriate biotinylated secondary antibodies, and then incubated with the streptavidin/horseradish peroxidase complex. The signal was visualized as the red reaction product of a 3-amino-9-ethyl carbazole liquid substrate chromogen (AEC, DAKO JAPAN Co., Ltd, Kyoto, Japan). To confirm the specificity of

Table I
Information respecting the deployment of the 52 rabbits used in this study

	Number of rabbits				Total number
	Group I	Group II	Group III	Group IV	
Materials					
IP-CHA	+	+	+	–	
rhBMP-2	+	–	–	–	
PLA–PEG	+	+	–	–	
Follow-up time					
1 week	4	0	0	0	4
3 weeks	6	6	6	6	24
6 weeks	6	6	6	6	24
Total number	16	12	12	12	52

Table II
*Histological scoring system**

Category	Points
Cell morphology	
Hyaline cartilage	4
Mostly hyaline cartilage	3
Mostly fibrocartilage	2
Mostly non-cartilage	1
Non-cartilage only	0
Matrix-staining (metachromasia)	
Normal	3
Slightly reduced	2
Markedly reduced	1
No metachromatic staining	0
Structural integrity	
Normal	2
Slight disruption	1
Severe disintegration	0
Surface regularity†	
Smooth	3
Moderate	2
Irregular	1
Severely irregular	0
Thickness of cartilage, %	
121–150	1
81–120	2
51–80	1
0–50	0
Regenerated subchondral bone	
Good	2
Moderate	1
Poor	0
Integration with adjacent cartilage	
Both edges integrated	2
One edge integrated	1
Neither edge integrated	0
Total maximum	18

*A modified version of the system described by Wakitani *et al.*[8].
†Total smooth area of repair cartilage compared with the entire area of the cartilaginous compartment of the defect.

the antibody under the adopted conditions and to confirm the specificity of the markers in target cells, all antibodies were tested for their reactivity in control tissues.

HISTOLOGICAL SCORING

To quantify the histological repair of articular cartilage defects, we employed a modified version of the grading scale described by Wakitani *et al.*[8]. This consists of seven categories and assigns a score ranging from 0 to 18 points (Table II). The following parameters were assessed: cell morphology (hyaline cartilage); metachromatic staining of the cartilage matrix; structural integrity of the regenerated cartilage; surface regularity of the tissue; thickness of the cartilage layer; regeneration of the subchondral bone; and integration of the tissue with adjacent cartilage.

STATISTICAL ANALYSES

Data pertaining to ALP activity were analyzed using an unpaired Student's *t* test. The histological scoring data were analyzed using the Kruskal–Wallis test, with a *post hoc* Bonferroni correction for non-parametric data.

Results

EVALUATION OF THE IMPLANTS

Scanning electron microscopy of IP-CHA samples revealed these to have a finely organized three-dimensional structure. Most of the IP-CHA pores were spherical, of similar size (approximately 100–200 μm in diameter) and uniformly interconnected via channels [10–80 μm in diameter; Fig. 1(B, C)]. Scanning electron microscopy of the BMP/PLA–PEG/IP-CHA composite revealed the BMP/PLA–PEG component to affect neither the pore size nor the interconnecting pore structure and to coat well the surface of the IP-CHA [Fig. 1(D, E)].

IN VITRO RELEASE KINETICS OF RHBMP-2 AND *IN VIVO* BIOASSAY FOR THE BMP/PLA–PEG/IP-CHA COMPOSITE

Based on ELISA, the BMP/PLA–PEG/IP-CHA composite released significant quantities of rhBMP-2 during the 21-day monitoring period [6.85 ± 1.31 μg/ml on day 1, 0.79 ± 0.22 μg/ml on day 3, 22.9 ± 0.62 ng/ml on day 7, 4.76 ± 1.13 ng/ml on day 14, and 2.71 ± 0.70 ng/ml on day 21; Fig. 2(A)].

To assess the bioactivity of the BMP/PLA–PEG/IP-CHA composites maintained *in vitro* for 0, 7 or 21 days, we implanted these, as well as IP-CHAs (control for the absence of rhBMP-2) within the back muscles of male ICR mice (a standard ectopic bone-formation model) and then analyzed the explanted material for its ALP activity. High levels of ALP activity could be detected even on day 21 [Fig. 2(B)], which accords with the rhBMP-2 release kinetics results *in vitro*.

MACROSCOPIC OBSERVATIONS OF CARTILAGE DEFECTS

Three weeks after implantation, the repaired defects in group I had a macroscopically smooth and glistening appearance and exhibited continuity with the surrounding host cartilage [Fig. 3(A)]. The controls (groups II–IV) revealed varying degrees of cartilage resurfacing with fibrous tissue [Fig. 3(B–D)].

At 6 weeks, the color and the glistening appearance of the repaired defects in group I were similar to those manifested by the adjacent host cartilage. The junction between the repaired tissue and the surrounding host cartilage was not clearly visible [Fig. 3(E)]. In contrast, the regenerated tissue in the control groups (groups II–IV) was

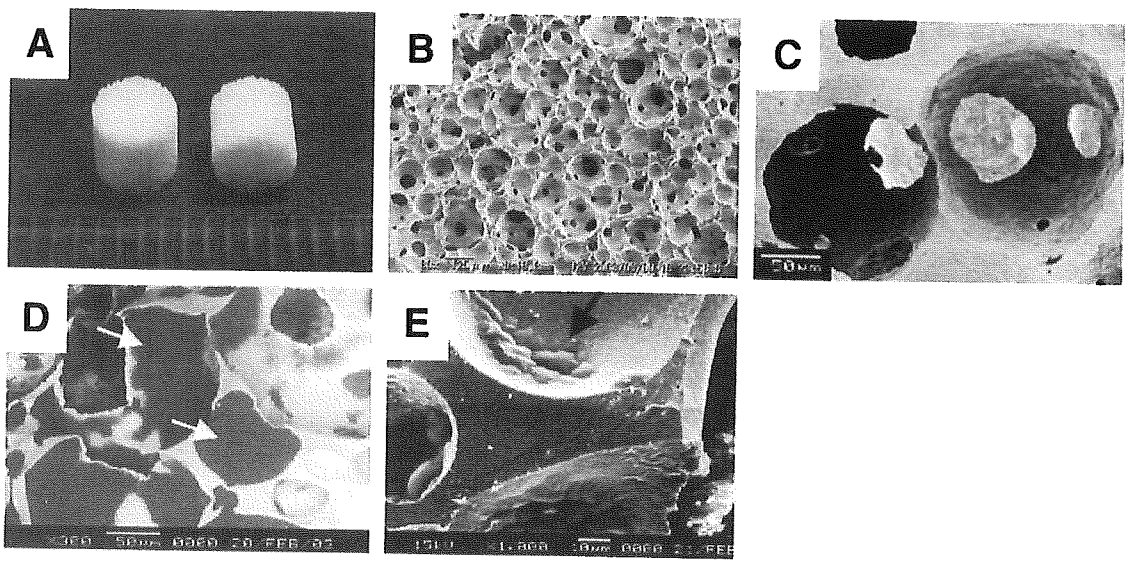

Fig. 1. Macroscopic photograph (A) and scanning electron micrographs (B–E) of IP-CHA specimens (4 mm in diameter and 4 mm in height). (A) Macroscopically, the surface of IP-CHA is slightly rough compared with that of other commercial porous hydroxyapatite materials, owing to its regular porous structure. (B, C) Scanning electron micrographs of IP-CHA, illustrating the regular arrangement of pores which are of similar size (100–200 μm in diameter), uniformly connected with each other, and separated by thin walls. (B) = 80×; (C) = 600×. (D, E) Scanning electron micrographs of the BMP/PLA–PEG/IP-CHA composite. (D) The dark areas lining the pores (white arrows) represent the BMP/PLA–PEG component. The introduction of BMP/PLA–PEG had no effect on either the pore size or the interconnecting pore structure. (E) Higher magnification of the lining of a pore (black arrow), revealing it to be well coated with BMP/PLA–PEG. (D) = 300×; (E) = 1000×.

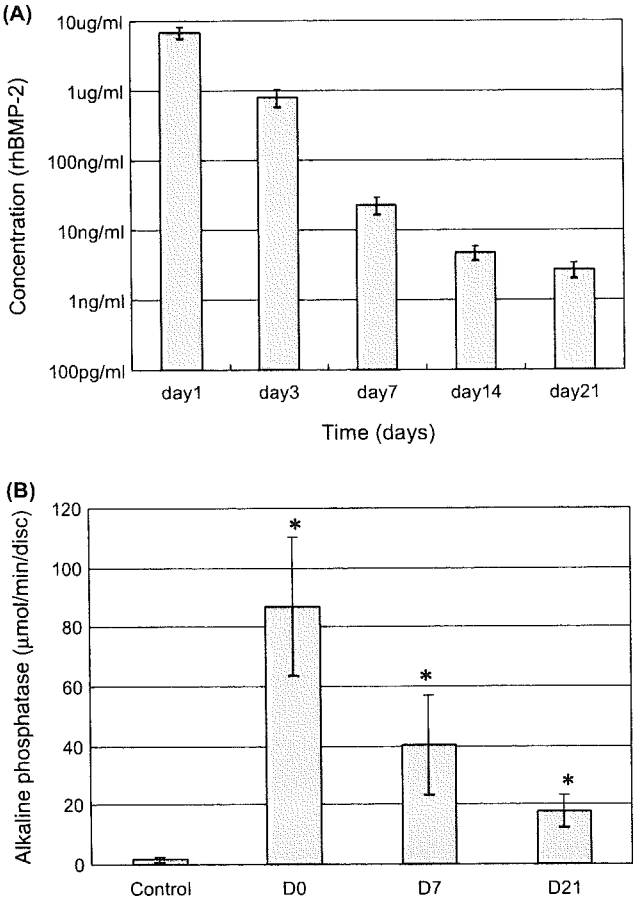

Fig. 2. Time course of rhBMP-2 release from the BMP/PLA–PEG/IP-CHA composite *in vitro* (A) and the bioactivity of the composites *in vivo* (B). (A) Release kinetics (measured by ELISA) of rhBMP-2 from the BMP/PLA–PEG/IP-CHA composite, illustrating significant quantities of rhBMP-2 during the 21-day monitoring period. The bar graph depicts the non-cumulative release at each time point. Mean values ± SD ($n = 4$) are represented. (B) The bioactivity of BMP/PLA–PEG/IP-CHA composites that were maintained *in vitro* for 0 (D0), 7 (D7), or 21 (D21) days was assessed 2 weeks after their implantation at an ectopic site in mice by monitoring the ALP activity of the explanted material. PLA–PEG/IP-CHA (no rhBMP-2) represented the control. High levels of ALP activity could be detected even on day 21 [86.8 ± 23.2 μmol/min/disc (day 0), 40.3 ± 16.8 μmol/min/disc (day 7), 17.7 ± 5.2 μmol/min/disc (day 21), 1.6 ± 0.8 μmol/min/disc (control)]. Mean values ± SD ($n = 4$) are represented. * = value is significantly different from the control ($P < 0.05$).

fibrous, and had a rough surface containing many fissures [Fig. 3(F–H)].

RADIOGRAPHIC EVALUATION

Six weeks after implantation, the soft X-ray analysis revealed defects treated with the BMP/PLA–PEG/IP-CHA composite (group I) to be consistently filled with newly formed bone, which was continuous with the surrounding intact subchondral bone [Fig. 3(I)]. In the control groups (groups II–IV), bone formation was incomplete and irregular [Fig. 3(J–L)].

HISTOLOGICAL EVALUATION

One week after implantation with the BMP/PLA–PEG/IP-CHA composite (group I), vigorous new bone formation was observed histologically within the pores of the IP-CHA scaffold [Fig. 4(B)], and about three-quarters of the defect depth above the IP-CHA had already been replaced with repair tissue. The central part of the repair tissue contained a fibrin clot and a few vessels. The lateral and lower regions consisted of granulation tissue, which was actively undergoing neovascularization and contained rounded fibroblast-like cells. These cells registered positive for Cbfa1 and/or CD105. They appeared to have infiltrated from the surrounding intact subchondral bone, either directly, or indirectly via the interconnecting IP-CHA pores, which were likewise filled with granulation tissue. Some of the pores in the peripheral 1-mm portions of IP-CHA blocks already contained newly formed bone (Fig. 4).

Three weeks after implantation with BMP/PLA–PEG/IP-CHA, the defect space above the IP-CHA blocks (subchondral space) was filled with newly generated and vigorous bone tissue, which penetrated the interconnecting pores of this material [Fig. 5(A, F)]. The regenerated articular cartilage was more cellular and contained less extracellular matrix than normal cartilage. The regenerated cartilage was divided into three distinct zones: (1) a superficial one, which contained flattened hyperchromatic cells; (2) a middle one, which contained rounded chondrocytes; and (3) a zone of enchondral ossification. The cartilage-like layer was two-to-three times thicker than normal cartilage [Fig. 5(A, E)]. In each of the control groups (groups II–IV), the regenerated fibrous cartilage had a similar morphological appearance, irrespective of the absence or presence of an implant. Although the subchondral space in group II tended to be filled with more newly formed bone than did that in the other control groups (groups III and IV), the quantitative histological evaluation revealed no significant difference between them [Table III; Fig. 5(B–D)].

Six weeks after implantation, defects treated with the BMP/PLA–PEG/IP-CHA composite (group I) were filled with regenerated subchondral bone, which also penetrated the pores of the implant. The subchondral bone was covered with a layer of regenerated cartilage tissue of almost normal thickness. The hyaline nature of the cartilage was maintained, and the tissue was beginning to assume a columnar organization and a horizontal stratification into four distinct zones (superficial, middle, deep and calcified), as in normal cartilage [Fig. 6(A, E)]. Interestingly, no gaps could be distinguished microscopically between the host cartilage and the newly regenerated cartilage, which suggests that the tissues were functionally and biologically integrated [Fig. 6(F)]. Safranin-O staining was evident predominantly in the middle and deep zones. Immunoreactivity for type-II collagen tended to be weakest in the deep zone at the junction with host tissue. But generally, the matrix exhibited a hyaline-like cartilaginous phenotype [registering negative for type-I collagen; Fig. 6(J–L)]. In contrast, defects in the control groups (groups II–IV) were filled with a hypercellular type of fibrous tissue. No hyaline cartilage was detected, despite the presence of new bone above and within the implant; [Fig. 6(B–D, G–I)]. Histological sections were assessed quantitatively using a modified version of an established grading system, which measures the degree and quality of cartilage repair[8] (Table II). At each time point, the scores for the BMP/PLA–PEG/IP-CHA composite (group I) were significantly better than those for groups II, III and IV ($P < 0.01$). These findings accord with the macroscopic and histological observations.

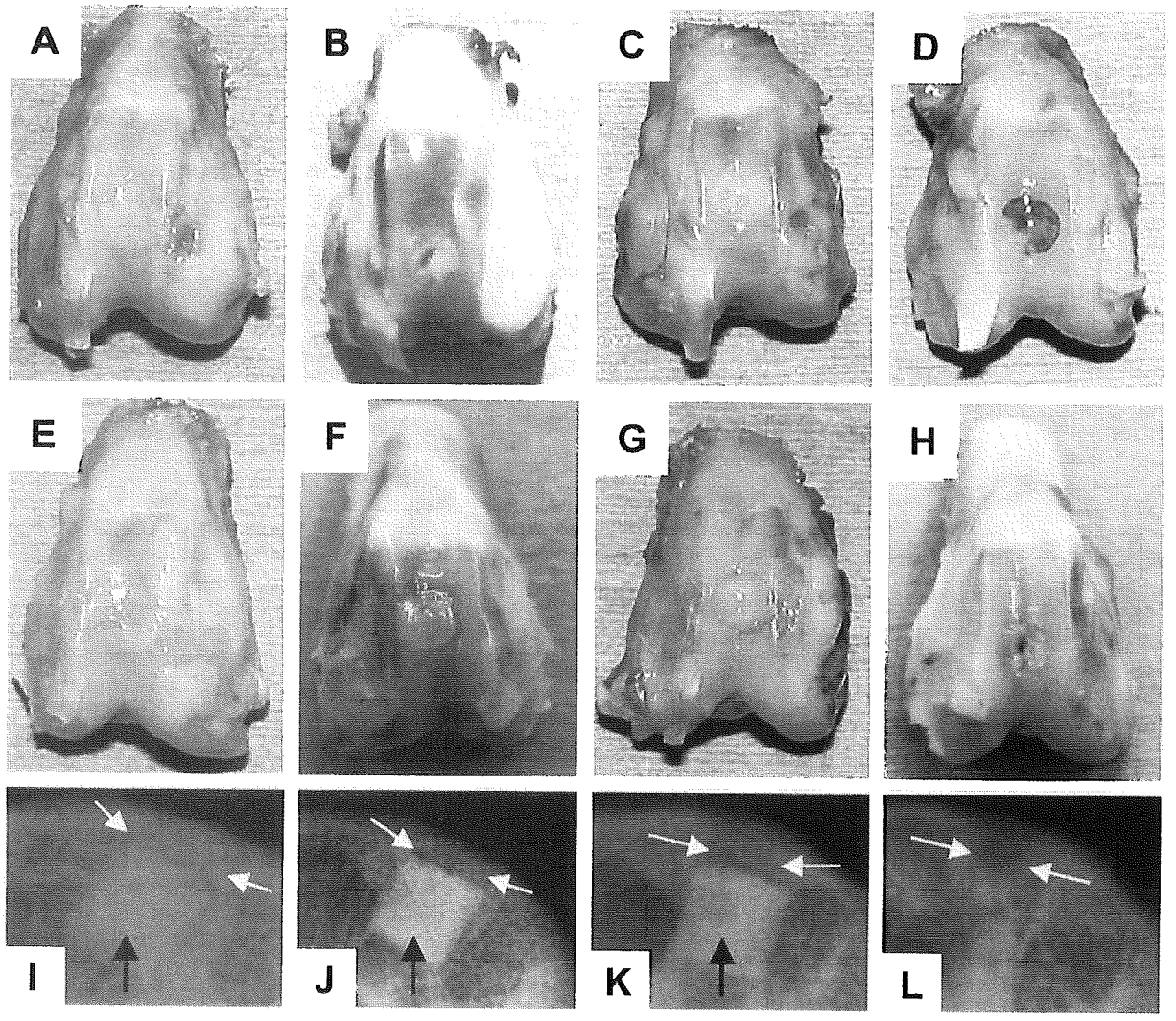

Fig. 3. Gross appearance (A–H) and soft X-ray photographs (I–L) of four specimens (one in each group) 3 weeks (A–D) and 6 weeks (E–L) after implantation. (A, E, I): BMP/PLA–PEG/IP-CHA composite (group I). (B, F, J): PLA–PEG/IP-CHA composite (group II). (C, G, K): IP-CHA alone (group III). (D, H, L): no implant (group IV). (A, E) In group I, reconstruction of the surface was good. At 3 weeks, the surface was still a little "white"; but at 6 weeks, it was smooth and glistening and exhibited continuity with the surrounding intact host cartilage. These macroscopic findings correspond with the histological results (Table III). (B, F) In group II, the articular cartilage defects were covered with "white" fibrous tissue with many fissures. (C, G) In group III, the regeneration of the defect looked better than those of other control groups (group II and IV), whereas the junction of the defects were still visible. (D, H) In group IV, in which the defects were left empty, at 3 weeks the defects were filled with red, semitransparent tissue with the margins sharply defined and the edges completely discernible (D). At 6 weeks, the defects were filled with irregular "white" tissue with pin-hole like fissure (H). (I–L) Representative soft X-ray photographs of the four specimens. The black arrows denote the implanted IP-CHA block. The white arrows above the IP-CHA block indicate the region where subchondral bone should be regenerated. A white, radiodense zone was observed above the IP-CHA block in group I (I); it denotes a vigorous regeneration of subchondral bone. This radiodense zone was not detected in groups II–IV (J–L).

Discussion

Several investigators have reported on the repair of articular cartilage defects using diverse tissue-engineering approaches. These include a gene-enhanced technique, the direct implantation of growth factors, and *in vitro* cell expansion[39–42]. BMPs have been shown to induce the differentiation of MSCs into chondrocytes both *in vitro* and *in vivo*. BMPs (BMP-2 and BMP-7) have also been used in conjunction with type-I collagen sponges to elicit the repair of osteochondral defects[43–45]. Cook *et al.*[40] have reported that type-I collagen sponges impregnated with rhBMP-7 can induce the repair of full-thickness osteochondral defects with hyaline-like cartilage in a dog model. The hyaline-like quality of the repair cartilage was still evident 52 weeks after surgery and the tissue had undergone no significant degradation. Sellers *et al.*[41] have demonstrated the capacity of rhBMP-2 to accelerate the healing of full-thickness articular cartilage defects and to improve the histological appearance and the biochemical characteristics of the repair cartilage. However, the tissue still differed from normal hyaline cartilage, both biochemically and structurally, and a long time elapsed before the defect area was completely filled with it. These suboptimal results probably reflect a limited recruitment of MSCs and/or a restricted delivery of cytokines, owing to the poor structural

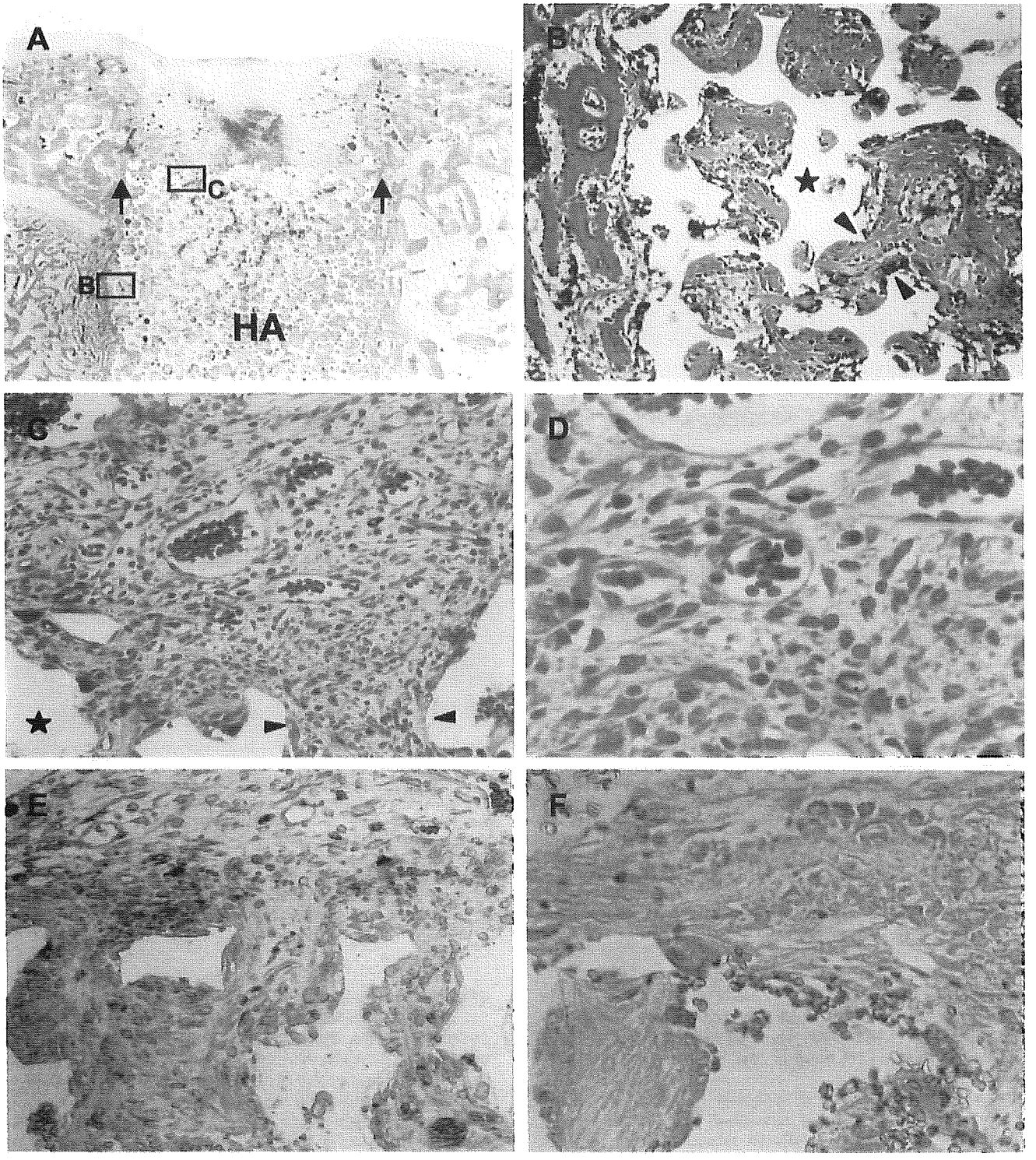

Fig. 4. Histological photomicrographs of a defect 1 week after the implantation of a BMP/PLA–PEG/IP-CHA composite (group I). (A) Overview of the defect site, the margins of which are indicated by arrows. HA represents the implanted IP-CHA scaffold (H&E). (B) Higher magnification of the region indicated in (A). The surface of newly formed bone trabeculae are lined with numerous cuboidal osteoblasts which have migrated from the neighboring host bone. (C) Higher magnification of the region indicated in (A), illustrating a neovascularized aggregate of cells which have migrated from the neighboring bone marrow, either directly or indirectly via the interconnecting channels of the IP-CHA composite. The arrowheads in (B) and (C) indicate the interconnecting pores of the IP-CHA scaffold. The asterisks denote regions that were occupied by hydroxyapatite before decalcification. (D) Higher magnification of (C), illustrating the rounded, fibroblast-like form of the aggregated cells. (E, F) Immunostaining of the aggregated cells for Cbfa1 (E) and CD105 (F). Many of the cells expressed the chondro/osteoblastic marker (E) and/or the mesenchymal one (F). Magnification: (A) = 10×; (B, C) = 100×; (E, F) = 200×; (D) = 400×.

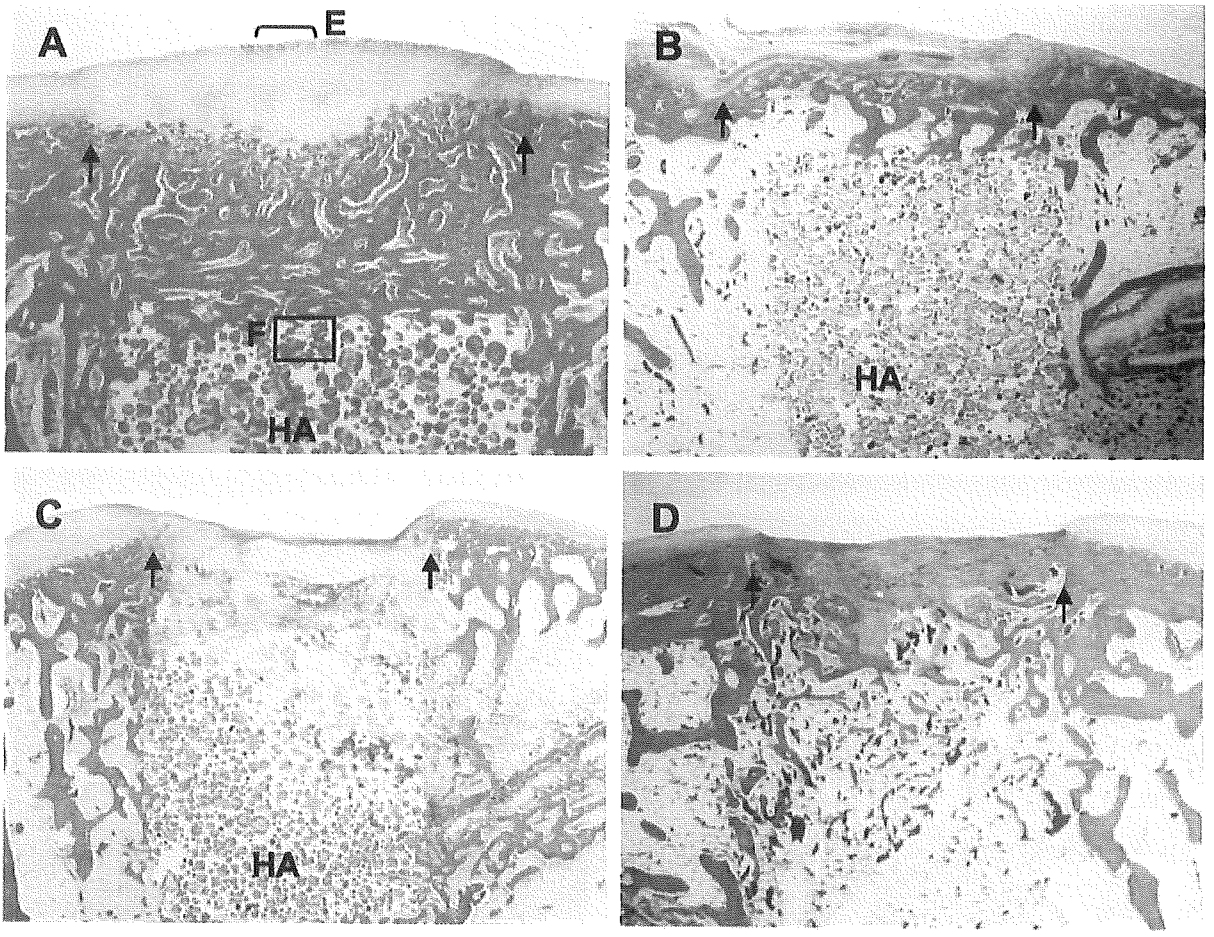

Fig. 5. Histological photomicrographs of defects (H&E staining) 3 weeks after implantation with either the BMP/PLA–PEG/IP-CHA composite [(group I) A, E, F], the PLA–PEG/IP-CHA composite [(group II) B], or IP-CHA alone [(group III) C], and in the absence of treatment [empty (group IV) D]. Arrows indicate the margins of the defect. HA represents the implanted IP-CHA scaffold. Highly magnified images of the regions indicated in (A) are represented in (E) and (F). (A) Section of a defect filled with the BMP/PLA–PEG/IP-CHA composite (group I), illustrating well-organized hyaline-like cartilage and accelerated replacement of vigorous subchondral bone. (B–D) In each of the control groups (group II–IV), the regenerated tissue had a similar morphological appearance, irrespective of the absence or presence of an implant. The defect site was filled predominantly with a hypocellular fibrocartilage repair tissue with incomplete replacement of subchondral bone. (E) The regenerated articular cartilage was more cellular and contained less extracellular matrix than normal cartilage. However, a stratified structure similar to normal cartilage was already visible. (F) Vigorous regeneration of subchondral bone occurred, which was carried up through the interconnections of the IP-CHA scaffold (arrowheads). The asterisk denotes a region that was occupied by hydroxyapatite before decalcification. Magnification: (A–D) = 10×; (E, F) = 100×.

organization of the supporting scaffold. The purpose of the present study was to evaluate the potential of IP-CHA to serve as a scaffold for the repair of full-thickness articular cartilage defects. This material has a well-organized interpore connectivity.

The osteoconductivity of polymer implants containing rhBMP-2 has been studied extensively[28,46]. In the present study, we used the synthetic bioabsorbable polymer PLA–PEG as a carrier for rhBMP-2. *In vitro*, rhBMP-2 was released continuously from the BMP/PLA–PEG/IP-CHA composite over a period of 21 days, as determined by ELISA [Fig. 2(A)]. This finding accords with the results of the *in vivo* bioassay [Fig. 2(B)], which was based on the ALP activity of composites implanted at an ectopic site in mice. However, it is of course conceivable that the release profile of rhBMP-2 at this ectopic site in mice differs greatly from that at the orthotopic site in our rabbit model.

Our new strategy for articular cartilage repair appears to be unique in three respects: (1) autogenous MSCs were efficiently recruited from the bone marrow by strongly activating regeneration within the subchondral bone compartment of the defect; (2) a sustained BMP stimulus appears to promote not only the vigorous regeneration of subchondral bone but also the ensuing differentiation of chondrocytes and the production of a cartilaginous matrix at the surface, which results in the regeneration of a hyaline-like cartilage layer in as short a time as 3 weeks; and (3) the regenerated cartilage integrated almost perfectly with the surrounding host cartilage, probably because the entire regeneration process was conducted *in situ*, i.e., it did not involve an *in vitro* chondrocyte-culturing step.

It is not known why the thickness of the repaired articular cartilage corresponded so closely to that of the host articular cartilage, with no bony differentiation. But articular factors, such as oxygen tension, joint effusion and mechanical stress, as well as subchondral influences, may regulate the differentiation process. Although the regenerated cartilage present 6 weeks after surgery was